

Biofilm inhibitor taurolithocholic acid alters colony morphology, specialized metabolism, and virulence of *Pseudomonas aeruginosa*

Condren, Alanna R; Kahl, Lisa Juliane; Boelter, Gabriela; Kritikos, George; Banzhaf, Manuel; Dietrich, Lars E P; Sanchez, Laura M

DOI:

[10.1021/acsinfecdis.9b00424](https://doi.org/10.1021/acsinfecdis.9b00424)

License:

None: All rights reserved

Document Version

Peer reviewed version

Citation for published version (Harvard):

Condren, AR, Kahl, LJ, Boelter, G, Kritikos, G, Banzhaf, M, Dietrich, LEP & Sanchez, LM 2020, 'Biofilm inhibitor taurolithocholic acid alters colony morphology, specialized metabolism, and virulence of *Pseudomonas aeruginosa*', *ACS Infectious Diseases*, vol. 6, no. 4, pp. 603-612. <https://doi.org/10.1021/acsinfecdis.9b00424>

[Link to publication on Research at Birmingham portal](#)

Publisher Rights Statement:

This document is the Accepted Manuscript version of a Published Work that appeared in final form in *ACS Infectious Diseases*, copyright © American Chemical Society after peer review and technical editing by the publisher. To access the final edited and published work see: <https://doi.org/10.1021/acsinfecdis.9b00424>

General rights

Unless a licence is specified above, all rights (including copyright and moral rights) in this document are retained by the authors and/or the copyright holders. The express permission of the copyright holder must be obtained for any use of this material other than for purposes permitted by law.

- Users may freely distribute the URL that is used to identify this publication.
- Users may download and/or print one copy of the publication from the University of Birmingham research portal for the purpose of private study or non-commercial research.
- User may use extracts from the document in line with the concept of 'fair dealing' under the Copyright, Designs and Patents Act 1988 (?)
- Users may not further distribute the material nor use it for the purposes of commercial gain.

Where a licence is displayed above, please note the terms and conditions of the licence govern your use of this document.

When citing, please reference the published version.

Take down policy

While the University of Birmingham exercises care and attention in making items available there are rare occasions when an item has been uploaded in error or has been deemed to be commercially or otherwise sensitive.

If you believe that this is the case for this document, please contact UBIRA@lists.bham.ac.uk providing details and we will remove access to the work immediately and investigate.

1 **Title**

2 Biofilm inhibitor tauroolithocholic acid alters colony morphology, specialized metabolism, and
3 virulence of *Pseudomonas aeruginosa*

4

5 **Short Title**

6 Biofilm inhibition alters colony morphology, specialized metabolism, and virulence of *P.*
7 *aeruginosa*

8

9 **Authors**

10 Alanna R. Condren¹, Lisa Juliane Kahl², Gabriela Boelter³, George Kritikos³, Manuel Banzhaf³,
11 Lars E. P. Dietrich², and Laura M. Sanchez^{1*}

12

13 **Affiliations**

14 1. Department of Pharmaceutical Sciences, University of Illinois at Chicago, Chicago, IL

15 60612

16 2. Department of Biological Sciences, Columbia University, New York, NY 10027

17 3. Institute of Microbiology & Infection and School of Biosciences, University of Birmingham,

18 Edgbaston, Birmingham, UK.

19 **Author Contributions**

20 Wrote the paper: ARC, LK, GB, GK, MB, LD, LMS

21 Conceptualized the research: ARC, LMS

22 Conducted the experiments: ARC, LK, MB, GK, GB

23 Provided strains: LK, LD

24 Supervised the research: MB, LD, LMS

25 **Correspondence**

26 sanchelm@uic.edu

27

28 **Abstract**

29 Biofilm inhibition by exogenous molecules has been an attractive strategy for the development
30 of novel therapeutics. We investigated the biofilm inhibitor tauroolithocholic acid (TLCA) and its
31 effects on the specialized metabolism, virulence and biofilm formation of the clinically relevant
32 bacterium *Pseudomonas aeruginosa* strain PA14. Our study shows that TLCA alters specialized
33 metabolism, thereby affecting *P. aeruginosa* colony biofilm physiology. We observed an
34 upregulation of metabolites correlated to virulence such as the siderophore pyochelin. A wax
35 moth virulence assay confirmed that treatment with TLCA increases virulence of *P. aeruginosa*.
36 Based on our results, we believe that future endeavors to identify biofilm inhibitors must
37 consider how a putative lead is altering the specialized metabolism of a bacterial community to
38 prevent pathogens from entering a highly virulent state.

39 **Keywords:** biofilms, tauroolithocholic acid, bile acid, *Pseudomonas aeruginosa*, virulence

40

41 The ESKAPE pathogens (*Enterococcus faecium*, *Staphylococcus aureus*, *Klebsiella*
42 *pneumoniae*, *Acinetobacter baumannii*, *Pseudomonas aeruginosa*, and *Enterobacter* species)
43 have been deemed a severe threat, as the major cause of nosocomial infections, by evolving
44 mechanisms to “escape” the biocidal action of antibiotics.^{1,2} The Center for Disease Control and
45 Prevention estimates that costs related to nosocomial infections, which have increased in
46 frequency in all countries regardless of income or industrial development, are between \$680 to
47 \$5,683 USD on average per patient.³

48 *P. aeruginosa*, one of the ESKAPE microorganisms, is often referred to as a “ubiquitous”
49 bacterium because of its ability to adapt to a wide variety of environments and hosts.⁴ *P.*
50 *aeruginosa* can be found in the lung of cystic fibrosis patients, colonizing large open wounds of
51 burn victims in hospitals, or invading the cornea of the human eye leading to permanent vision
52 loss.⁵⁻⁷ *P. aeruginosa* infections are often complicated by the fact that it readily forms a
53 multicellular aggregate known as a biofilm - a state which contributes towards its resistance to
54 antibiotics.⁸ The minimum bactericidal concentration for cells in a biofilm state is estimated to be
55 10-1000 times higher than their planktonic counterparts complicating treatment of biofilm
56 infections.⁹ Yet, there are currently no biofilm inhibitors on the market in the US.¹⁰

57 There are, however, several biofilm inhibitors used for *in vitro* analysis of biofilm
58 dispersal.¹¹ One example is tauro lithocholic acid (TLCA), a bile acid which efficiently inhibits
59 biofilm formation and induces dispersion of mature *P. aeruginosa* biofilms.^{12,13} TLCA
60 demonstrated a low micromolar biofilm inhibitory concentration (BIC₅₀) against *P. aeruginosa* at
61 38.4 μ M compared to other lithocholic and bile acid derivatives.¹² Bile acids are a class of acidic
62 steroids that play a physiological role in digestion by solubilizing dietary fats.¹⁴ Though bile acids
63 are classified as detergents, the steroid control cholesterol 3-sulfate, does not inhibit biofilm
64 formation nor do other bile acids tested at concentrations up to 1 mM. However, all lithocholic bile
65 acids have specific bioactivity against *P. aeruginosa* which varies based on the conjugation to
66 glycine or taurine.¹² Additionally, the reported BIC₅₀ of TLCA was in the low micromolar range

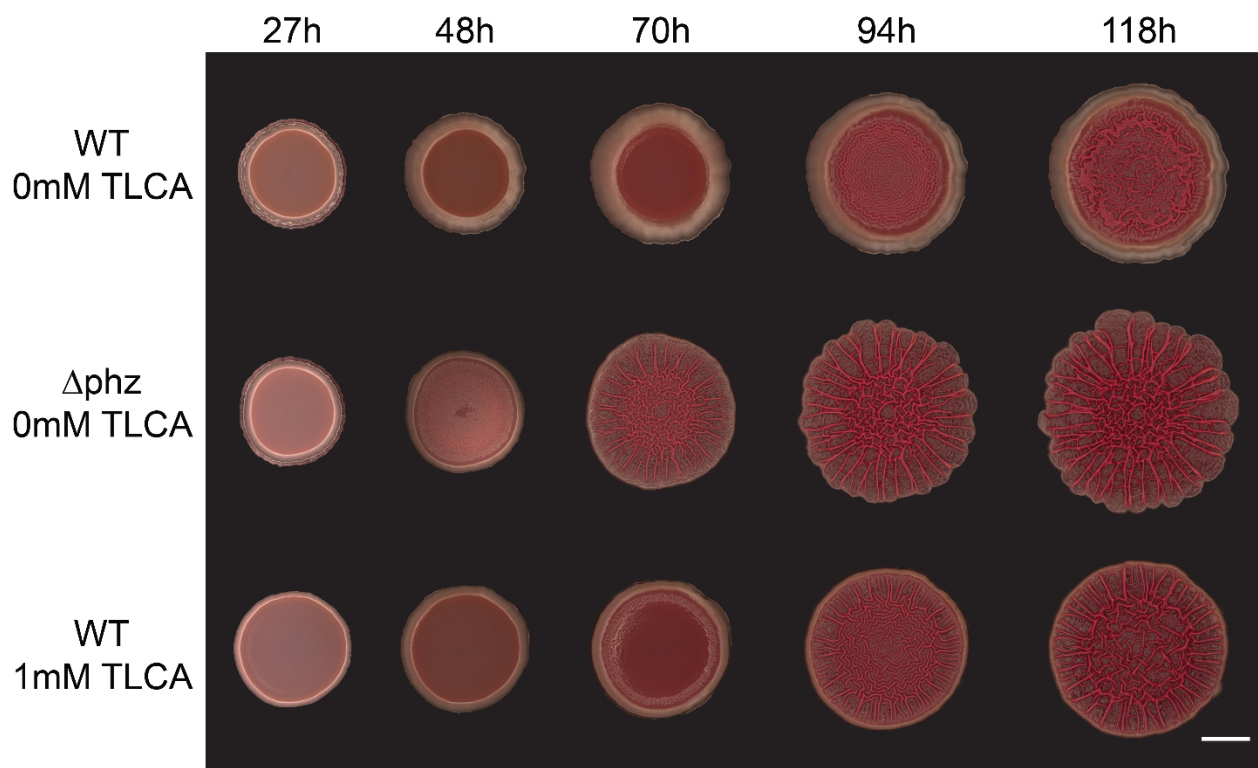
67 while the maximum critical micelle concentration for these bile acids ranges from 8 to 12 mM.¹⁴
68 *P. aeruginosa* tightly regulates biofilm formation using molecular signaling networks and a well-
69 characterized arsenal of specialized metabolites.^{15–19} Therefore, we hypothesized that TLCA
70 treatment induces *P. aeruginosa* to alter the production of specific specialized metabolites leading
71 to the reported biofilm inhibition/dispersion.

72 We observed altered morphology of colony biofilms and changes in specialized
73 metabolism when *P. aeruginosa* PA14 is exposed to TLCA. An increase in pyochelin production
74 when TLCA is present lead us to perform a wax moth virulence model which confirmed that TLCA
75 treated cells are significantly more virulent than non-treated cells.²⁰ The observed increase in
76 virulence led to an investigation into how TLCA may be inducing an increase in virulence factors
77 such as pyochelin. We performed an iron starvation tolerance assay as well as mutant studies via
78 imaging mass spectrometry (IMS) which concluded that TLCA treatment does not make *P.*
79 *aeruginosa* cells sensitive to iron starvation and a knockout of the *pqsH* ($\Delta pqsH$) and *phzA1-G1*
80 *phzA2-G2* (Δphz) gene clusters also leads to an increase in pyochelin production as observed for
81 the wild-type strain.²¹ Taken together, while TLCA has shown promising bioactivity towards biofilm
82 inhibition, it appears that biofilm inhibition (or dispersion) ultimately leads to the bacterium
83 becoming more virulent in a host model, which is supported by the observed alteration in
84 specialized metabolism.

85 **Results & Discussion**

86 Phenazines constitute one of the most notable families of specialized metabolites
87 produced by *P. aeruginosa*. Phenazines are redox-active compounds that have been implicated
88 in balancing redox homeostasis in the hypoxic regions of biofilms, thereby regulating biofilm
89 morphology.^{22–26} A phenazine-null mutant (Δphz) over produces extracellular matrix which causes
90 Δphz mutant biofilms to have a characteristic hyper wrinkled morphology that allows for increased

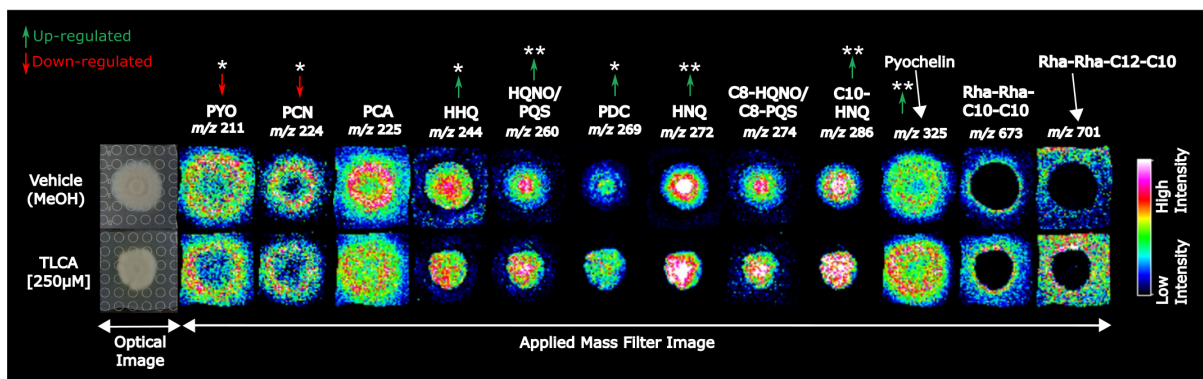
91 access to oxygen due to a higher surface area-to-volume ratio.²⁶⁻²⁹ To characterize the effect of
92 TLCA on *P. aeruginosa* biofilms, we grew PA14 colonies in a colony morphology assay on solid
93 agar supplemented with Congo Red, Coomassie Blue, and TLCA (0, 100, 250, and 1000 μ M) for
94 five days (**Figure S1**). Wild type PA14 initially forms a smooth colony but initiates wrinkle structure
95 development after 70 h (**Figure 1**). In contrast, a Δ phz mutant showed enhanced production of
96 biofilm matrix, leading to an earlier onset of wrinkling between 24 and 48 h. Addition of TLCA to
97 the medium promoted a hyper-wrinkled morphology after 94 h. The colony continued to wrinkle
98 over time, resembling the Δ phz mutant (118 h; **Figure 1**). This morphology phenotype was also
99 observed at lower concentrations, but it was most dramatic at 1 mM TLCA, which is a
100 physiologically relevant concentration (**Figure S1**).³⁰ Based on this assay, it appears that TLCA
101 induces matrix production, possibly by downregulating phenazines.



102

103 **Figure 1: The effect of TLCA on colony biofilm formation in *P. aeruginosa* PA14.** After five
104 days of growth, colonies that were exposed to TLCA showed a similar hyper-wrinkled biofilm
105 structure to that of the untreated Δ phz mutant. (N =3)

106 The putative decrease in phenazine production as indicated by the Δphz -like colony
107 morphology in the presence of TLCA was queried alongside other changes in specialized
108 metabolism using imaging mass spectrometry (IMS). We employed matrix-assisted laser
109 desorption/ionization time-of-flight IMS (MALDI-TOF IMS), because it provides a robust,
110 untargeted analysis of the specialized metabolites produced by *P. aeruginosa in situ*.^{31,32} *P.*
111 *aeruginosa* colonies were grown on thin agar (2-3 mm) with the vehicle or 250 μ M of TLCA for 48
112 h. The colonies and their respective agar controls were then prepared for IMS analysis. Twelve
113 known specialized metabolites were identified and visualized from *P. aeruginosa* colonies (**Figure**
114 **2**). Orthogonal analytical techniques were used to confirm identities of all twelve metabolites
115 (**Figure S2**). Following a combination of manual and statistical analyses using SCiLS lab, eight
116 of the twelve specialized metabolites were observed to have significant altered regulation in the
117 presence of TLCA ($p < 0.05$; **Table S1**). The specialized metabolites represent four broad classes
118 of molecular families including the phenazines, quinolones, rhamnolipids, and siderophores. We
119 found that the phenazines pyocyanin (PYO) and phenazine-1-carboxamide (PCN) are
120 significantly downregulated when TLCA is present, supporting our hypothesis that TLCA exposure
121 causes hyper-wrinkled colonies by downregulating phenazine production. We did not observe a
122 statistically significant change in phenazine-1-carboxylic acid (PCA) production in the presence
123 of TLCA. Since N-methylated phenazines like PYO were shown to inhibit colony wrinkling our
124 data is consistent with TLCA affecting colony morphology by modulating phenazine production.³³



125

126 **Figure 2: MALDI-TOF IMS analysis of *P. aeruginosa* after exposure to TLCA.**

127 Twelve specialized metabolites produced by *P. aeruginosa* were identified and visualized. Signal
 128 intensity is displayed as a heat map and shows that exposure to TLCA altered regulation of
 129 highlighted specialized metabolites compared to control. * denotes the signal is significantly up-
 130 or down-regulated in two biological replicates within the colony and ** denotes the signal was
 131 significant over all three biological replicates ($p < 0.05$).

132 *P. aeruginosa* is reported to produce up to 50 quinolones which are specialized
 133 metabolites that play specific roles in signaling and/or virulence. For example, both 2-heptyl-4-
 134 quinolone (HHQ) and *Pseudomonas* quinolone signal (PQS) are specifically known for their
 135 signaling properties but have also demonstrated antifungal bioactivity.^{34–40} The N-oxide quinolone,
 136 4-hydroxy-2-heptylquinoline-N-oxide (HQNO), has recently been shown to have antimicrobial
 137 activity towards Gram-positive bacteria and contributes to *P. aeruginosa*'s virulence.^{34–39} When
 138 *P. aeruginosa* was treated with TLCA, we observed a significant upregulation of HHQ, PQS, and
 139 4-hydroxy-2-nonylquinoline (HNQ) in the *P. aeruginosa* colony. PQS is a well-characterized
 140 signaling molecule in *P. aeruginosa* quorum sensing cascade.⁴¹ Though IMS is a valuable tool for
 141 identifying and visualizing the chemical composition of a sample, it cannot differentiate between
 142 constitutional isomers like HQNO and PQS (m/z 260; **Figure 2**). In order to differentiate these two
 143 metabolites, we used a combination of tandem mass spectrometry and knockout mutants to
 144 demonstrate that PQS was represented by the signal that is retained in the colony (center,
 145 upregulated) and HQNO corresponds to the signal that was excreted into the agar (outer signal,
 146 downregulated). HHQ and PQS are well established signaling molecules that are required for

147 phenazine production in *Pseudomonas aeruginosa*, However, since we observed decreased
148 phenazine levels despite an increase in quinolone production⁴² our results suggest that TLCA is
149 attenuating phenazine production in a quinolone-independent manner.

150 Based on the IMS analyses, treatment of TLCA seems to induce the production of
151 biosurfactants. Surfactants, such as rhamnolipids, are amphipathic small molecules that *P.*
152 *aeruginosa* produces to increase surface adhesion and motility.⁴³ Rha-Rha-C10-C10 and Rha-
153 Rha-C12-C10/C10-C12 production were produced at elevated levels after treatment with TLCA
154 (**Figure 2**). However, while the upregulation was not determined to be statistically significant
155 overall biological replicates, the trend observed is worth noting. In colony biofilms, TLCA markedly
156 increases matrix production and leads to increased spreading and wrinkling. This wrinkly spreader
157 phenotype is reminiscent of the phenazine-null mutant as seen in **Figure 1**.

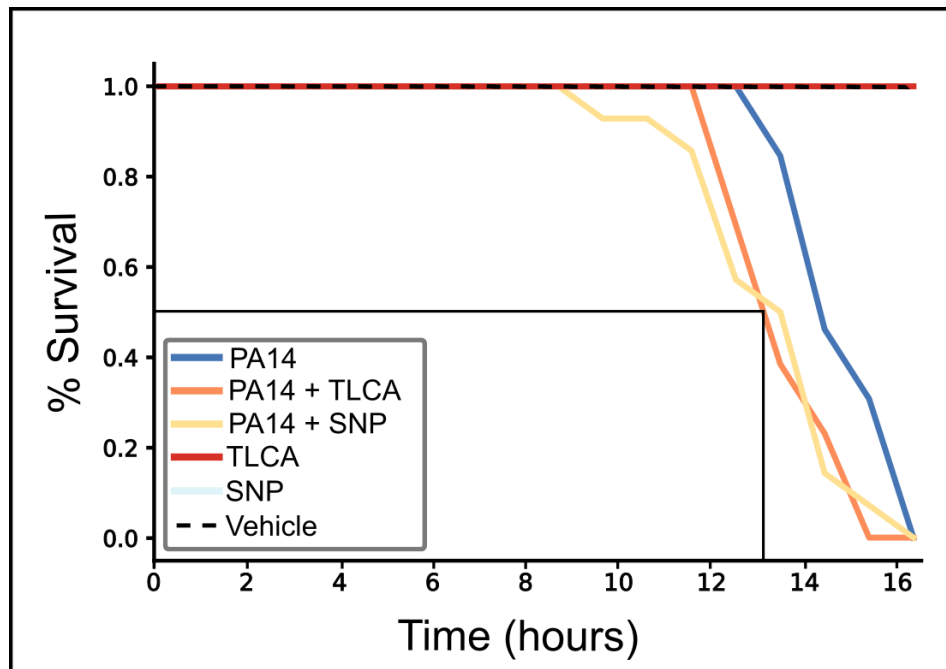
158 In addition to quinolones and phenazines, we detected changes in the levels of the
159 siderophore pyochelin. Siderophores are iron chelators that allow bacteria to acquire iron from
160 the surrounding environment.⁴⁴ Siderophores have been known to sequester iron from host
161 proteins and simultaneously act as signals for biofilm development.¹⁷ The IMS results show a
162 significant upregulation of pyochelin in the presence of TLCA (**Figure 2**). Pyochelin is produced
163 by the biosynthetic pathway *pchA-I* which is activated by the presence of both iron and the ferric
164 uptake regulator (Fur).¹⁷ Additionally, previous work has shown that an increase in iron-bound
165 PQS can indirectly increase siderophore production by activating the siderophore gene clusters
166 *pvd* and *pch*; our IMS experiments with TLCA treatment of wild-type PA14 are in line with these
167 results (**Figure 2**).⁴⁵ Siderophores have antimicrobial activity and contribute to virulence.^{46,47}
168 Hence, the TLCA-dependent upregulation of pyochelin raised the question of whether TLCA-
169 exposed *P. aeruginosa* become hypervirulent.

170 Many bacteria, like the ESKAPE pathogens, exhibit distinct lifestyle states depending on
171 surrounding environmental factors. Chua *et al.* recently described characteristics of the dispersed

172 cell state using sodium nitroprusside (SNP) as a biofilm-dispersing agent.²¹ They found that
173 dispersed cells are characterized by altered physiology, increased virulence against
174 macrophages and *C. elegans*, and extreme sensitivity to iron starvation.²¹ Having observed an
175 increase in pyochelin production when exposing *P. aeruginosa* to TLCA (**Figure 2**), we sought to
176 determine if TLCA treated cells were hypervirulent using a *Galleria mellonella* (greater wax moth)
177 larvae virulence assay.

178 *G. mellonella* larvae have been shown to be an ideal model for studying microbial
179 pathogenesis of several ESKAPE pathogens since they are easily infected, inexpensive, and
180 produce a similar immune response as vertebrates and mammals.^{48–52} In the *G. mellonella* model,
181 the potency of treatment is measured via a Kaplan-Meier curve, therefore a shift at the 50%
182 survival rate compared to the appropriate control will indicate increased or decreased virulence
183 of *P. aeruginosa*.⁵³ To observe how TLCA and SNP treatment altered virulence of *P. aeruginosa*
184 infected larvae, TLCA or SNP were injected with *P. aeruginosa* and larvae survival was monitored
185 for 25 h. Treatment of uninfected larvae with either SNP or TLCA did not affect larvae survival
186 (**Figure 3; Table S2**). Within 15 h, 50% of larvae infected with *P. aeruginosa* succumbed to
187 infection and treatment with SNP or TLCA led to a significant decrease in survival with 50% of the
188 larvae succumbing to infection 2 h earlier than the infected control group (**Figure 3**; $p < 0.05$).
189 These results indicate that TLCA treatment increases virulence, mimicking what was previously
190 reported from SNP treatment.²² Given the high dose of TLCA administered we also sought to
191 control for an immunological response. Larvae were treated with taurocholic acid (TCA), a
192 derivative of TLCA which has been previously shown to have no biofilm inhibition against *P.*
193 *aeruginosa*.¹⁸ Treatment with TCA altered survival slightly however only TLCA treatment caused
194 a significant increase in virulence compared to control group (**Figure S3A**). This suggests that
195 treatment with bile acids induces an innate immunological response but the observed increase in
196 virulence from TLCA treatment is significant compared to TCA treatment or control group.

197 In continuing to explore how specialized metabolites impact virulence, we used the Δphz
198 mutant in the wax moth assay. We observed the Δphz mutant takes longer than WT to reduce
199 the population to 50%, therefore, the Δphz mutant is intrinsically less virulent (**Figure S3B**).
200 TLCA treatment of the Δphz mutant infected larvae induce a significant increase in virulence
201 compared to the control (**Figure S3B**; $p < 0.05$), however, TCA treatment induced the same
202 increase in virulence. This similarity in response to both bile acids indicates that the observed
203 shift in the survival curve of the Δphz mutant is due to an immunological response from the bile
204 acids. Based on our *in vivo* assays, WT PA14 cells treated with TLCA are significantly more
205 virulent, and TLCA treatment is linked to specialized metabolism since the increase in virulence
206 was lost when the Δphz mutant was tested.



207

208 **Figure 3: Virulence assay with *Galleria mellonella* (greater wax moth).** Using *G. mellonella*
209 as an infection model revealed that regardless of agent (250 μ M), WT PA14 treated cells show a
210 significant increase in virulence compared to controls (N=3).

211 In a previous report, SNP-dispersed *P. aeruginosa* PAO1 cells resulted in decreased
212 production of the siderophore pyoverdine and also showed a sensitivity to iron starvation when

213 competing with exogenous iron chelator DIPY.²² We were unable to detect pyoverdine in either
214 the wild type or TLCA-treated *P. aeruginosa* PA14 via mass spectrometry, but we were able to
215 detect pyochelin in our IMS experiments which Chua *et al.* did not measure (**Figure 2**). Having
216 confirmed that TLCA treatment increases virulence in *P. aeruginosa*, we next tested whether *P.*
217 *aeruginosa* TLCA-treated cells would also be sensitive to iron stress due to increased pyochelin
218 production. Therefore, we recapitulated the iron starvation assay performed by Chua *et al.* to
219 determine if TLCA exposure induced sensitivity to iron starvation as shown previously for SNP-
220 dispersed cells.

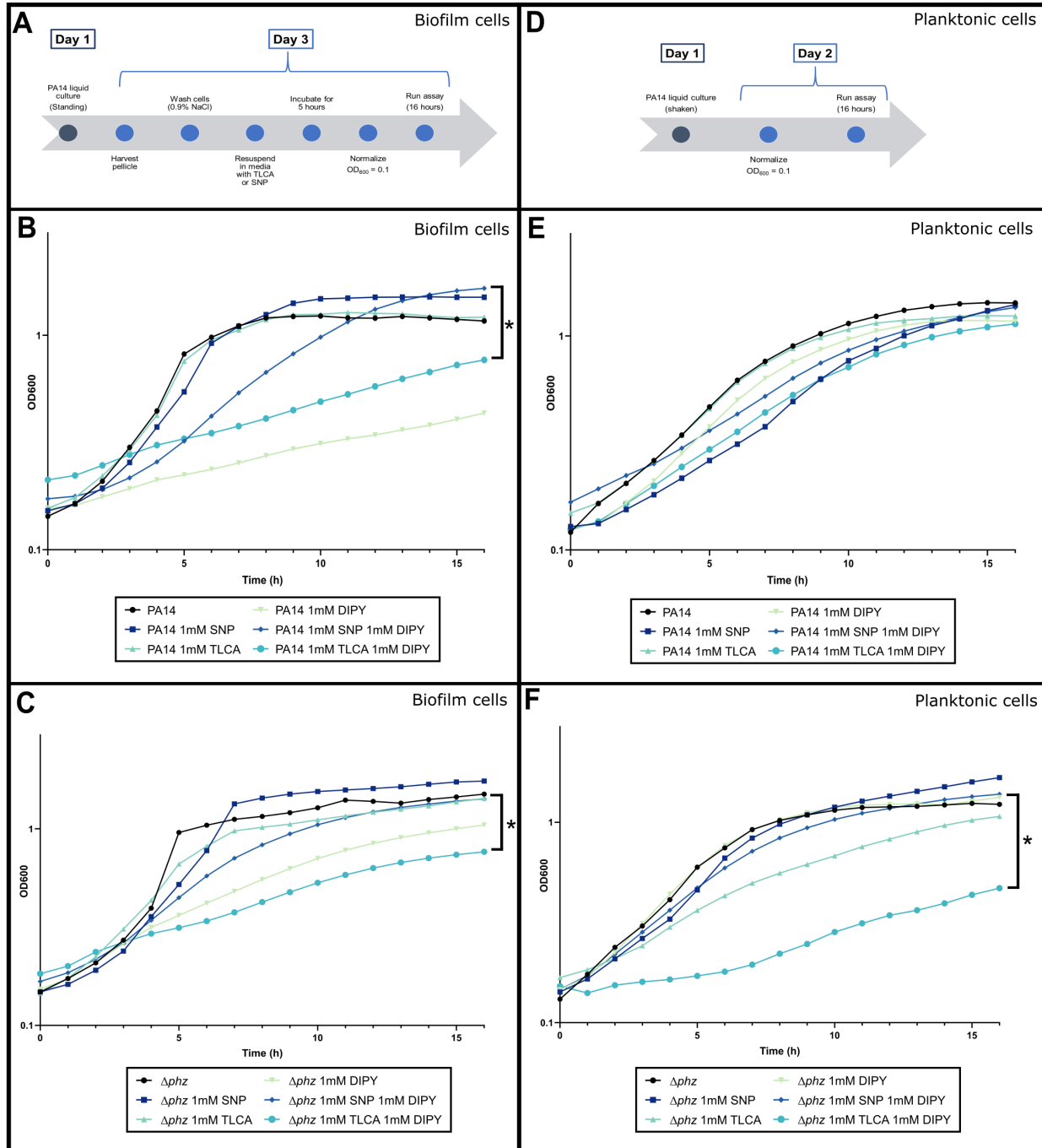
221 Iron starvation was induced by exposing PA14 cells to the iron chelator 2'2-bipyridine
222 (DIPY; **Figure 4**). This assay was performed with TLCA or SNP treated cells, which were
223 generated using two different methods: 1) from pellicles (biofilms grown at the air-liquid interface
224 in standing liquid cultures; **Figure 4A-C**), and 2) planktonic cells (shaken liquid cultures; **Figure**
225 **4D-F**). Treatment of *P. aeruginosa* PA14 with either TLCA or SNP does not alter proliferation
226 compared to the DIPY control (**Figure 4B**). Regardless of agent used for treatment, *P. aeruginosa*
227 PA14 cells do not show an increase in sensitivity to iron starvation (**Figure S4**). Therefore, TLCA
228 and SNP treatment does not increase *P. aeruginosa* PA14's sensitivity to iron starvation. The
229 same trend occurred with *P. aeruginosa* PA14 Δphz (**Figure 4C**).

230 Using WT PA14 planktonic cells, we observe no change in growth regardless of condition
231 (**Figure 4E**). Interestingly, TLCA treatment of the Δphz mutant planktonic cells showed a
232 significant increase in sensitivity compared to SNP treated cells (**Figure 4F**). Based on our data,
233 dispersed biofilm cells and WT planktonic cells show no sensitivity to iron starvation. However,
234 planktonic cells of the Δphz mutant show significant sensitivity when biofilm formation is inhibited
235 via TLCA treatment. This result agrees with our hypothesis that TLCA is altering the specialized
236 metabolism of PA14 and phenazines may help alleviate sensitivity to iron starvation during TLCA
237 treatment since phenazines are capable of carrying oxidation and reduction of iron species to

238 increase bioavailability.²⁷ With our previous morphology assay and IMS experiments, the iron
239 starvation assay confirms that TLCA treatment likely effects the phenazine production which leads
240 to altered morphology and metabolism in response to biofilm inhibition from an exogenous small
241 molecule treatment.

242 Of note, we do not observe the same sensitivity of SNP treatment with iron starvation as
243 reported by Chua *et al.* which is likely due to the difference in strains used for this assay (PA14
244 vs PAO1). The discrepancy in iron starvation sensitivity between SNP and TLCA might be
245 attributed to different pyoverdine production capabilities of these strains. Though we were unable
246 to detect pyoverdine in our IMS analysis, we would speculate that iron starvation might be
247 prevented by the increased production of pyochelin in colony biofilms that were treated with TLCA
248 (**Figure 2**). Despite their differing effects on iron starvation sensitivity, both SNP and TLCA have
249 previously been shown to readily disperse biofilms, likely through different mechanisms of
250 action.^{18,22} SNP, a nitric oxide donor, has been shown to disperse mature biofilms by producing
251 nitrosative stress inside of the biofilm structure.²¹ Since TLCA cannot act as a nitric oxide donor
252 and it does not cause cell lysis, TLCA must act via an alternative mechanism to disperse
253 biofilms.¹⁸ This supports our hypothesis that TLCA's bioactivity is achieved through inducing
254 changes in *P. aeruginosa*'s specialized metabolism.

255



256

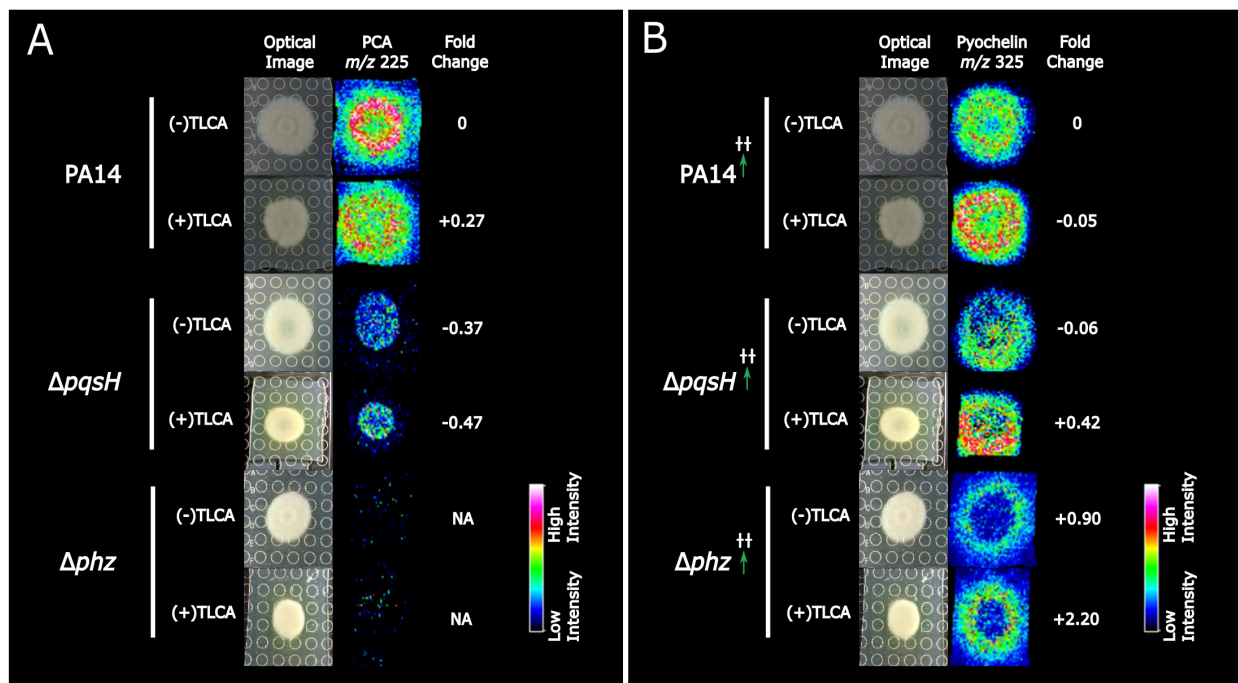
257 **Figure 4: PA14 Iron starvation assay.** (A) Experimental workflow for collection and dispersion
 258 of PA14 biofilm cells. (B) Starvation of iron via exposure to DIPY showed that TLCA dispersed
 259 cells are more sensitive to iron starvation than SNP dispersed cells. However, cells dispersed
 260 with either agent are not more sensitive to iron starvation when compared to DIPY control. (C)
 261 The Δphz mutant dispersed cells hold the same trend with no significant change in sensitivity from
 262 TLCA or SNP treatment. (D) Experimental workflow for the preparation of planktonic cells. (E)

263 Planktonic PA14 cells also show no sensitivity to iron starvation regardless of agent used. (F)
264 Interestingly, treatment of the Δphz mutant with TLCA lead to a significant increase in sensitivity
265 to iron starvation and the population was unable to fully recover over the 16 hour experiment. *
266 denotes $p < 0.05$.

267
268 PQS is a major quorum sensing signal and iron-bound PQS upregulates siderophore
269 production.⁴⁵ The increase in pyochelin production *in situ* and the enhanced virulence *in vivo* lead
270 us to investigate the contribution of the *pqs* gene cluster to the TLCA-mediated effect. We tested
271 four mutants with deletions in quinolone and phenazine biosynthetic genes: $\Delta pqsA-C$, $\Delta pqsH$,
272 $\Delta pqsL$, and Δphz . $\Delta pqsA-C$ does not produce any quinolones, while $\Delta pqsH$ cannot produce PQS
273 and $\Delta pqsL$ cannot produce N-oxide quinolones such as HQNO.^{42,48,49} The phenazine-null mutant,
274 Δphz , is a double-deletion of the two redundant core phenazine biosynthetic gene clusters *phzA1-*
275 *G1* and *phzA2-G2*.^{42,48,49} Using IMS, we investigated if any of the four mutants would recapitulate
276 the TLCA-dependent increase in pyochelin production that we observed for the WT. No variation
277 in pyochelin production for $\Delta pqsA-C$ and $\Delta pqsL$ mutants was found, while $\Delta pqsH$ mutant
278 produced significantly more pyochelin in response to TLCA, mimicking the trend observed in the
279 WT ($p < 0.05$; **Figure S5**). This result puts into question our earlier assumption that PQS and
280 pyochelin production are positively correlated. We also observed a significant increase in
281 pyochelin production in the Δphz mutant (**Figure S5**). Previous work has shown that increasing
282 PCA concentrations allows PA14 siderophore-null mutants to still develop biofilms and sequester
283 iron.⁵⁰ This may be due to phenazine's ability to mediate the reduction of Fe(III) to the bioavailable
284 Fe(II).⁵⁰ *pqsH* and *phz* gene clusters are necessary for phenazine production, hence a decrease
285 or lack of phenazine production caused by TLCA treatment might be responsible for the observed
286 increase in pyochelin production (**Figures 2 & S5**).

287 Since our IMS results were inconclusive regarding the effect of TLCA on PCA production
288 in colony biofilms (**Figure 2**), we subjected bacterial colony extracts from wild-type PA14, $\Delta pqsH$,
289 and the Δphz mutant to an HPLC analysis to measure fold change across biological (N=3) and
290 technical replicates (n=3) (**Figure 5A**). When considering fold changes greater than +/- 1, PCA

291 production was not altered by TLCA exposure in the wild type and $\Delta pq s H$ strains (not produced
 292 by the $\Delta p h z$ mutant). When monitoring pyochelin production, only TLCA treatment of the $\Delta p h z$
 293 mutant showed a fold change increase in pyochelin production compared to control (+2.20)
 294 (Figure 5B). When the $\Delta pq s H$ mutant is complemented ($\Delta pq s H::pq s H$) there is increased
 295 production of pyochelin compared to the wild-type regardless of whether the colony is TLCA-
 296 treated or not (Table S10). There was no notable difference in production of pyochelin in the
 297 complementation strain whether it was TLCA-treated or not, which recapitulates the wild-type
 298 data. Though the fold change of PCA and pyochelin was comparable in both wild-type PA14 and
 299 $\Delta pq s H$, the change in the production of these two metabolites in the phenazine-null mutant, $\Delta p h z$,
 300 suggests that a lack of phenazine production is correlated to the observed increase in pyochelin
 301 production from cells exposed to TLCA.
 302

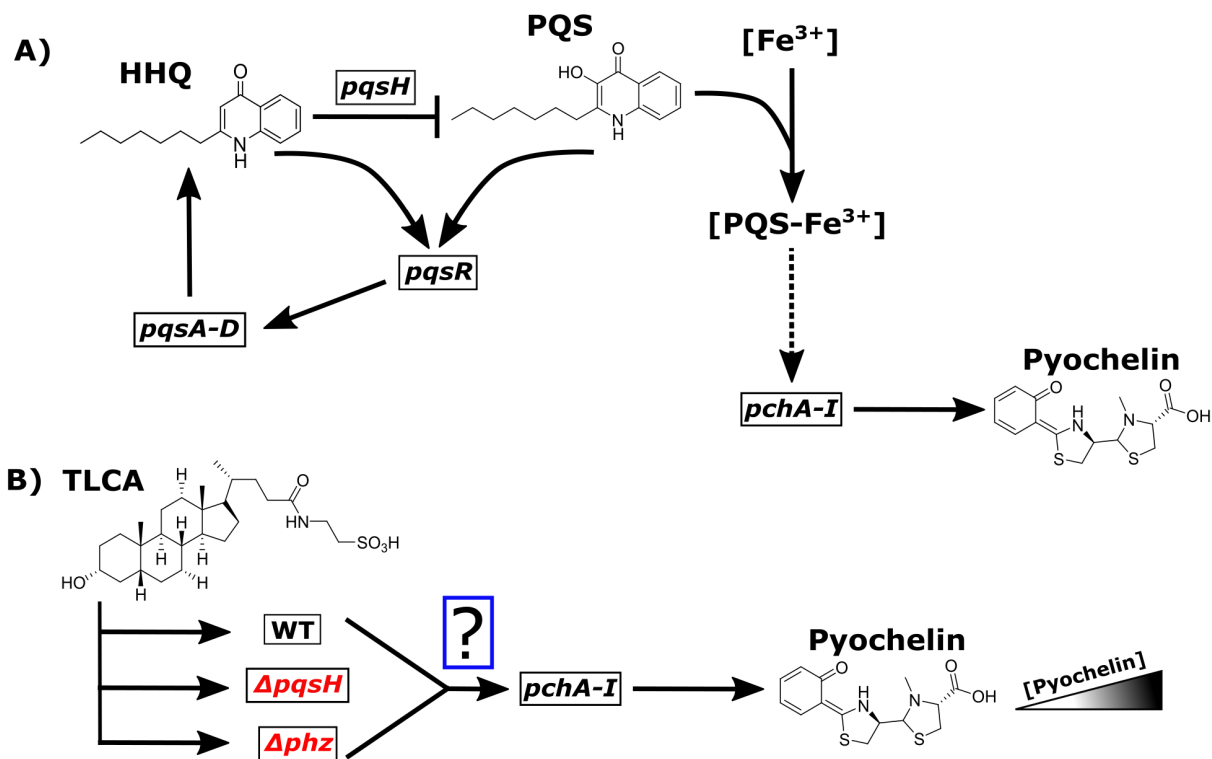


303
 304 **Figure 5: IMS and fold change analysis of wild type PA14, $\Delta pq s H$, and $\Delta p h z$ mutants.** (A)
 305 IMS and HPLC fold-change analysis revealed a 250 μ M treatment of TLCA induced no change in
 306 PCA production however (B) there was an increase in pyochelin production in the $\Delta p h z$ mutant,
 307 resembling the trend observed in WT. †† denotes the observed regulation was statistically

308 significant over three biological replicates in IMS experiments ($p < 0.05$).
309

310 **Conclusion**

311 In this study we demonstrate that the mammalian endogenous enteric metabolite, TLCA, can alter
312 colony morphology, specialized metabolism, and virulence of *P. aeruginosa*. Our biological and
313 chemical studies confirm what is already known about TLCA's bioactivity and offers insight into
314 the chemical communication occurring between the cells upon treatment with a known biofilm
315 inhibitor. TLCA-treated cells are not sensitive to iron starvation, as previously reported for the
316 biofilm-dispersing agent SNP, however treatment with either agent induces a significant increase
317 in virulence *in vivo*, implying that the mechanism of action of the two biofilm inhibitors is different.
318 Our IMS analysis of mutant strains revealed that when exposed to TLCA, a lack of PQS ($\Delta pqsH$)
319 or phenazine production (Δphz) lead to an increase in pyochelin production, matching the results
320 observed in our colony morphology and IMS WT experiments. Therefore, PQS or iron-bound PQS
321 is not responsible for activating the *pchA-I* gene cluster (**Figure 6A**). However, IMS analysis
322 highlighted that a significant increase in pyochelin production was observed in the Δphz mutant
323 confirming that TLCA treatment not only affects phenazine production but could also play a role
324 in the observed increased pyochelin production when TLCA is present (**Figure 6B**). Though these
325 results are not conclusive regarding the mechanism of TLCA since biofilm inhibition and dispersal
326 cannot be tested using colony biofilms as a model system, it does support the hypothesis that
327 TLCA is acting as an environmental cue to induce *P. aeruginosa* to alter its metabolic signaling
328 throughout the bacterial community.



329

330 **Figure 6: pqs metabolic pathway under TLCA exposure.** (A) Represents the canonical
 331 pathway for pyochelin production with the role iron-bound PQS plays in indirectly (dashed-line)
 332 activating pyochelin production. (B) However, TLCA treatment of the WT or ΔpqsH, and Δphz
 333 mutants leads to an increase in pyochelin production and subsequently virulence supporting that
 334 these genes play a role in the observed increase in pyochelin production from TLCA exposure.
 335

336 More work is needed to determine the mechanism of action of TLCA, but our work shows
 337 that through TLCA-treated *P. aeruginosa* bacterial communities increase the production of
 338 virulence factors, such as pyochelin, *in vitro* and induced hypervirulence *in vivo*. Others have
 339 documented similar phenomena by reporting an increase in virulence *in vivo* as a consequence
 340 of treatment with a biofilm inhibitor in organisms such as, Group A *Streptococcus*, *Vibrio cholerae*,
 341 and *Candida albicans*.⁵¹⁻⁵⁵ Based on previous literature, our work supports that future
 342 investigations should measure the chemical environment within a biofilm, and that biofilm
 343 inhibition as a treatment strategy should be closely monitored for undesired side effects, such as
 344 increased virulence.

345 **Experimental Section**

346 *TLCA stock solution preparation.* Tauroolithocholic acid was purchased from Sigma Aldrich
347 ($\geq 98\%$). A 0.5 M stock solution was made by dissolving TLCA in methanol. This solution was then
348 sterile filtered with a 0.22 μm sterile filter and stored at -80°C .

349 *Colony Morphology Studies.* Liquid agar was prepared by autoclaving 1% tryptone (Teknova), 1%
350 agar (Teknova) mixture. The liquid agar was cooled to 60°C and Congo Red (EMD; final
351 concentration 40 $\mu\text{g}/\text{mL}$) and Coomassie Blue (EMD; final concentration: 20 $\mu\text{g}/\text{mL}$) were added.
352 TLCA stock solution, dissolved in MeOH, was vortexed for 2-3 min until clear. TLCA was added
353 to liquid agar, different amounts were added to reach the final concentrations of 100 μM , 250 μM ,
354 and 1 mM TLCA. 60 mL of liquid agar mixture was poured into square plates (LDP, 10 cm x 10
355 cm x 1.5 cm) and left to solidify for ~ 18 -24 h. Precultures of *P. aeruginosa* PA14 were grown in
356 LB for 12-16 h at 37°C while shaking at 250 rpm. Subcultures were prepared as 1:100 dilutions
357 of precultures into fresh LB media and shaking for 2.5 h at 37°C , at which point all subcultures
358 had reached mid-exponential phase (optical density of ~ 0.4 - 0.6 at 500 nm). Morphology plates
359 were dried for 20-30 min and 10 μL spots of subculture were spotted onto a morphology plate,
360 with not more than four colonies per plate. Colony biofilms were grown at 25°C and high humidity
361 ($+90\%$) for up to 5 d. Images were taken every 24 h with a Keyence VHX-1000 microscope.

362 *Imaging mass spectrometry experiments.* TLCA and the respective vehicle (MeOH) were added
363 into liquid agar prior to plating. LB agar was autoclaved and cooled to 55°C before adding TLCA.
364 The final concentration of TLCA in each agar plate was 250 μM . Plates were stored in 4°C
365 refrigerator until needed. *P. aeruginosa* PA14 was plated on Bacto LB agar and grown overnight
366 at 30°C . A colony from the plate was then used to inoculate a 5 mL LB liquid culture of *P.*
367 *aeruginosa* and grown overnight at 30°C shaking at 225 rpm. Overnight liquid cultures (5 μL) was
368 spotted on thin agar plates (10 mL of agar in 90 mm plate) embedded with either TLCA or the
369 vehicle (MeOH) and incubated for 48 h at 30°C . Humidity/moisture was removed from environment

370 during growth by placing a small amount of DrieRite in the incubator. Following 48 h of growth,
371 colonies were excised from agar plates using a razor blade and transferred to an MSP 96 target
372 ground steel target plate (Bruker Daltonics). An optical image of the colonies on the target plate
373 was taken prior to matrix application. A 53 μm stainless steel sieve (Hogentogler Inc) was used
374 to coat the steel target plate and colonies with MALDI matrix. The MALDI matrix used for the
375 analysis was a 1:1 mixture of recrystallized α -cyano-4-hydroxycinnamic acid (CHCA) and 2,5-
376 dihydroxybenzoic acid (DHB) (Sigma). The plate was then placed in an oven at 37°C for
377 approximately 4 h or until the agar was fully desiccated. After 4 h, excess matrix was removed
378 from target plate and sample with a stream of air. Another optical image was taken of the
379 desiccated colonies on the target plate. The target plate and desiccated colony were then
380 introduced into the MALDI-TOF mass spectrometer (Bruker Autoflex Speed) and analyzed with
381 FlexControl v.3.4 and FlexImaging v.4.1 software. The detector gain and laser power were set at
382 3.0 \times and 41% respectively. Range of detection was from 100 Da to 3,500 Da with ion suppression
383 set at 50 Da in positive reflectron mode. The raster size was set to 500 μm and the laser was set
384 to 200 shots per raster point at medium (3) laser size.

385 *Statistical analysis of Imaging Data.* SCiLS software (Bruker, version 2015b) was used to run
386 statistical analysis of raw imaging data. Settings for analysis was as follows: Normalization: root
387 mean square (RMS), error: ± 0.2 Da, and weak denoising for segmentation. Using “Find
388 Discriminative Values (ROC)” for unbiased analysis, PA14 control colony was selected as class
389 1 and TLCA treated colony as class 2 and SCiLS identified signals that were significantly
390 upregulated in class 1 (MeOH control colony) with a threshold of 0.75 corresponding to a Pearson
391 correlation of $p < 0.05$. In our report, these signals are referred to as “downregulated” since they

392 have a higher intensity in the control. The same analysis was performed with the classes flipped
393 to identify signals that were upregulated in TLCA condition. Statistical analysis was completed
394 after calculating mass error (**Table S3**) of three biological replicates (N=3) (**Figures S6S-8**) and
395 signals were only considered significant if altered regulation was observed in two or more
396 replicates.

397 *Iron Stress Tolerance Assay*: The protocol for the iron stress tolerance assay used was exactly
398 as described by Chua *et al.*,²¹ with the exceptions that strain PA14 rather than PAO1 and a 1 mM
399 of TLCA and 2'2-bipyridine (DIPY) were used. The OD at 600 nm of each liquid culture was
400 measured every 15 min for 16 h.

401 *Galleria mellonella treatment assays*. *Galleria mellonella* larvae (greater wax moth) were
402 purchased from TrueLarv UK Ltd. or Livefoods, UK and stored at 15°C prior to use. The assay
403 was performed as described previously,⁵⁶ except for the following differences: PA14 wild-type
404 (WT) cells were grown exponentially for 2 h, washed with PBS buffer and adjusted to an OD₍₆₀₀₎
405 of 0.1. The PA14 culture was further diluted with PBS and plated to determine the CFU of the
406 inoculation suspension. Larvae were inoculated with 20 µL of a 2.5 × 10³ CFU/mL solution and
407 20 µL of compound or PBS. The final concentration of TLCA and sodium nitroprusside (SNP) was
408 250 µM. For controls, uninfected larvae were administered the same compound dose to monitor
409 for toxicity. In parallel one group of larvae received sterile PBS injections to control for
410 unintentional killing by the injections. Survival of a larvae was determined by the ability to respond
411 to external stimuli (poking). To increase robustness of the *G. mellonella* treatment assay several,
412 independent experiments were pooled to draw conclusions. All raw data can be found in
413 supplementary data set 1 . Larvae survival was estimated using the Kaplan-Meier estimator.⁵⁷
414 Survival estimates were subsequently compared using the log-rank test.⁵⁸ Resulting p-values
415 were corrected using the Benjamini-Hochberg method (**Tables S2 & S4**).⁵⁹

416 *pqs mutants IMS analysis.* Mutants proceeded through the same protocol as the WT (PA14)
417 bacterial colonies . IMS sample prep and experimentation was completed at the same settings as
418 described in “Imaging mass spectrometry experiments” section. Statistical analysis was
419 completed after calculating mass error (**Table S5-S9**) of three biological replicates (N=3) and
420 signals were only considered significant if altered regulation was observed in two or more
421 replicates.

422 *PQS complementation.* The complementation strains *P. aeruginosa* PA14 $\Delta pqsA-C::pqsA-C$,
423 $\Delta pqsH::pqsH$, and $\Delta pqsL::pqsL$ were constructed as described in Jo *et al.* [57]. Primers LD1 &
424 LD4, LD168 & LD171, and LD9 & LD12 were used to amplify the *pqsA-C*, *pqsH* and *pqsL* genes,
425 respectively (**Table S10**). Correct constructs were confirmed by PCR and sequencing and
426 complemented into the original deletion site, following the same procedure as for deletion.

427 *Bacterial Extraction for PCA and PCH Fold-change.* Bacterial growth for quantification proceeded
428 exactly as described in “Imaging mass spectrometry experiments”. Each strain (PA14 WT, $\Delta pqsA-$
429 *C*, $\Delta pqsH$, Δphz , $\Delta pqsA-C::pqsA-C$, and $\Delta pqsH::pqsH$) was plated in duplicate. After 48 h,
430 colonies and surrounding agar were excised, transferred, and extracted with MeOH.. Total
431 weights of each sample dry extract was used to achieve a 10 mg/mL solution of each extract for
432 HPLC analysis (N=3, n=3).

433 *PCA and PCH Fold-change analysis.* PCA standard was purchased from ChemScence (>97%).
434 An HPLC method previously described by Adler *et al.* was used on an Agilent 1260 Infinity to
435 isolate and identify PCA through retention time matching with standard (32.5 min at 250 nm;
436 **Figure S9**) with a Phenomenex C18 analytical column (150 x 4.6 mm; 5 μ m) and a flow rate of
437 0.5 mL/min.⁶⁰ Area under the curve (AUC) was used to quantify fold-change between PA14 WT
438 and other strains/conditions. For PCH fold-change quantification, a gradient of 10%-85% ACN

439 (0.1% TFA) and H₂O (0.1% TFA) over 25 min with the two PCH stereoisomers (pyochelin I and
440 II) eluting at 16.0 & 16.2 min respectively at 210 nm (**Figure S10**). Area reported for fold change
441 analysis was achieved by combining the AUC of the peaks for pyochelin I and II. Fold-change
442 analysis was determined by averaging the AUC's from three independent biological cultures
443 (N=3), with three technical replicates (n=3), and compared to PA14 WT with no TLCA (control).

444 **Supporting information**

445 Materials and methods expanded information, strain information, molecular networking used to
446 verify the structures identified with imaging mass spectrometry, IMS replicates, fold change HPLC
447 analysis, mass error reports and statistical analysis reports, data availability.

448 **Acknowledgements**

449 We thank Drs. Atul Jain and Terry Moore for assisting with the recrystallization of the MALDI matrices,
450 Dr. Michael Federle for access to Biotek plate reader, and Dr M. Lisandra Zepeda Mendoza for
451 assistance with statistics. Funding was provided by Grant K12HD055892 from the National Institute
452 of Child Health and Human Development (NICHD) and the National Institutes of Health Office of
453 Research on Women's Health (ORWH) (L.M.S.); University of Illinois at Chicago Startup Funds
454 (L.M.S.); American Society for Pharmacognosy research startup grant (L.M.S.); NIH/NIAID grant
455 R01AI103369 and an NSF CAREER award (L.E.P.D). ARC was supported in part by the National
456 Science Foundation Illinois Louis Stokes Alliance for Minority Participation Bridge to the Doctorate
457 Fellowship (grant number 1500368) and a UIC Abraham Lincoln retention fellowship.

458 **References**

- 459 (1) Rice, L. B. Federal Funding for the Study of Antimicrobial Resistance in Nosocomial
460 Pathogens: No ESKAPE. *J. Infect. Dis.* **2008**, *197* (8), 1079–1081.
- 461 (2) Rice, L. B. Progress and Challenges in Implementing the Research on ESKAPE
462 Pathogens. *Infect. Control Hosp. Epidemiol.* **2010**, *31 Suppl 1*, S7–S10.
- 463 (3) Kouchak, F.; Askarian, M. Nosocomial Infections: The Definition Criteria. *Iran. J. Med.*
464 *Sci.* **2012**, *37* (2), 72–73.
- 465 (4) Kramer, A.; Schwebke, I.; Kampf, G. How Long Do Nosocomial Pathogens Persist on
466 Inanimate Surfaces? A Systematic Review. *BMC Infect. Dis.* **2006**, *6*, 130.
- 467 (5) Spencer, W. H. Pseudomonas Aeruginosa Infections of the Eye. *Calif. Med.* **1953**, *79*
468 (6), 438–443.
- 469 (6) Norbury, W.; Herndon, D. N.; Tanksley, J.; Jeschke, M. G.; Finnerty, C. C. Infection in

- 470 Burns. *Surg. Infect.* **2016**, *17* (2), 250–255.
- 471 (7) Finch, S.; McDonnell, M. J.; Abo-Leyah, H.; Aliberti, S.; Chalmers, J. D. A
472 Comprehensive Analysis of the Impact of *Pseudomonas Aeruginosa* Colonization on
473 Prognosis in Adult Bronchiectasis. *Ann. Am. Thorac. Soc.* **2015**, *12* (11), 1602–1611.
- 474 (8) Hall, C. W.; Hinz, A. J.; Gagnon, L. B.-P.; Zhang, L.; Nadeau, J.-P.; Copeland, S.; Saha,
475 B.; Mah, T.-F. *Pseudomonas Aeruginosa* Biofilm Antibiotic Resistance Gene *ndvB*
476 Expression Requires the RpoS Stationary-Phase Sigma Factor. *Appl. Environ. Microbiol.*
477 **2018**, *84* (7). <https://doi.org/10.1128/AEM.02762-17>.
- 478 (9) Wu, H.; Moser, C.; Wang, H.-Z.; Høiby, N.; Song, Z.-J. Strategies for Combating
479 Bacterial Biofilm Infections. *Int. J. Oral Sci.* **2015**, *7* (1), 1–7.
- 480 (10) Stewart, P. S. Prospects for Anti-Biofilm Pharmaceuticals. *Pharmaceuticals* **2015**, *8* (3),
481 504–511.
- 482 (11) Rabin, N.; Zheng, Y.; Opoku-Temeng, C.; Du, Y.; Bonsu, E.; Sintim, H. O. Agents That
483 Inhibit Bacterial Biofilm Formation. *Future Med. Chem.* **2015**, *7* (5), 647–671.
- 484 (12) Sanchez, L. M.; Cheng, A. T.; Warner, C. J. A.; Townsley, L.; Peach, K. C.; Navarro, G.;
485 Shikuma, N. J.; Bray, W. M.; Riener, R. M.; Yildiz, F. H.; et al. Biofilm Formation and
486 Detachment in Gram-Negative Pathogens Is Modulated by Select Bile Acids. *PLoS One*
487 **2016**, *11* (3), e0149603.
- 488 (13) Sanchez, L. M.; Wong, W. R.; Riener, R. M.; Schulze, C. J.; Linington, R. G. Examining
489 the Fish Microbiome: Vertebrate-Derived Bacteria as an Environmental Niche for the
490 Discovery of Unique Marine Natural Products. *PLoS One* **2012**, *7* (5), e35398.
- 491 (14) Monte, M. J.; Marin, J. J. G.; Antelo, A.; Vazquez-Tato, J. Bile Acids: Chemistry,
492 Physiology, and Pathophysiology. *World J. Gastroenterol.* **2009**, *15* (7), 804–816.
- 493 (15) Mukherjee, S.; Moustafa, D. A.; Stergioula, V.; Smith, C. D.; Goldberg, J. B.; Bassler, B.
494 L. The PqsE and RhIR Proteins Are an Autoinducer Synthase-Receptor Pair That
495 Control Virulence and Biofilm Development in *Pseudomonas Aeruginosa*. *Proc. Natl.*
496 *Acad. Sci. U. S. A.* **2018**, *115* (40), E9411–E9418.
- 497 (16) Heeb, S.; Fletcher, M. P.; Chhabra, S. R.; Diggle, S. P.; Williams, P.; Cámara, M.
498 Quinolones: From Antibiotics to Autoinducers. *FEMS Microbiol. Rev.* **2011**, *35* (2), 247–
499 274.
- 500 (17) Banin, E.; Vasil, M. L.; Greenberg, E. P. Iron and *Pseudomonas Aeruginosa* Biofilm
501 Formation. *Proc. Natl. Acad. Sci. U. S. A.* **2005**, *102* (31), 11076–11081.
- 502 (18) Cezairliyan, B.; Vinayavekhin, N.; Grenfell-Lee, D.; Yuen, G. J.; Saghatelian, A.;
503 Ausubel, F. M. Identification of *Pseudomonas Aeruginosa* Phenazines That Kill
504 *Caenorhabditis Elegans*. *PLoS Pathog.* **2013**, *9* (1), e1003101.
- 505 (19) Das, T.; Kutty, S. K.; Tavallaie, R.; Ibugo, A. I.; Panchompoo, J.; Sehar, S.; Aldous, L.;
506 Yeung, A. W. S.; Thomas, S. R.; Kumar, N.; et al. Phenazine Virulence Factor Binding to
507 Extracellular DNA Is Important for *Pseudomonas Aeruginosa* Biofilm Formation. *Sci.*
508 *Rep.* **2015**, *5*, 8398.
- 509 (20) Barraud, N.; Hasset, D. J.; Hwang, S.-H.; Rice, S. A.; Kjelleberg, S.; Webb, J. S.
510 Involvement of Nitric Oxide in Biofilm Dispersal of *Pseudomonas Aeruginosa*. *J.*
511 *Bacteriol.* **2006**, *188* (21), 7344–7353.
- 512 (21) Chua, S. L.; Liu, Y.; Yam, J. K. H.; Chen, Y.; Vejborg, R. M.; Tan, B. G. C.; Kjelleberg,
513 S.; Tolker-Nielsen, T.; Givskov, M.; Yang, L. Dispersed Cells Represent a Distinct Stage
514 in the Transition from Bacterial Biofilm to Planktonic Lifestyles. *Nat. Commun.* **2014**, *5*,
515 4462.
- 516 (22) Recinos, D. A.; Sekedat, M. D.; Hernandez, A.; Cohen, T. S.; Sakhtah, H.; Prince, A. S.;
517 Price-Whelan, A.; Dietrich, L. E. P. Redundant Phenazine Operons in *Pseudomonas*
518 *Aeruginosa* Exhibit Environment-Dependent Expression and Differential Roles in
519 Pathogenicity. *Proc. Natl. Acad. Sci. U. S. A.* **2012**, *109* (47), 19420–19425.
- 520 (23) Price-Whelan, A.; Dietrich, L. E. P.; Newman, D. K. Pyocyanin Alters Redox

- 521 Homeostasis and Carbon Flux through Central Metabolic Pathways in *Pseudomonas*
522 *Aeruginosa* PA14. *J. Bacteriol.* **2007**, *189* (17), 6372–6381.
- 523 (24) Price-Whelan, A.; Dietrich, L. E. P.; Newman, D. K. Rethinking “Secondary” Metabolism:
524 Physiological Roles for Phenazine Antibiotics. *Nat. Chem. Biol.* **2006**, *2* (2), 71–78.
- 525 (25) Mentel, M.; Ahuja, E. G.; Mavrodi, D. V.; Breinbauer, R.; Thomashow, L. S.;
526 Blankenfeldt, W. Of Two Make One: The Biosynthesis of Phenazines. *Chembiochem*
527 **2009**, *10* (14), 2295–2304.
- 528 (26) Okegbe, C.; Fields, B. L.; Cole, S. J.; Beierschmitt, C.; Morgan, C. J.; Price-Whelan, A.;
529 Stewart, R. C.; Lee, V. T.; Dietrich, L. E. P. Electron-Shuttling Antibiotics Structure
530 Bacterial Communities by Modulating Cellular Levels of c-Di-GMP. *Proc. Natl. Acad. Sci.*
531 *U. S. A.* **2017**, *114* (26), E5236–E5245.
- 532 (27) Briard, B.; Bomme, P.; Lechner, B. E.; Mislin, G. L. A.; Lair, V.; Prévost, M.-C.; Latgé, J.-
533 P.; Haas, H.; Beauvais, A. *Pseudomonas Aeruginosa* Manipulates Redox and Iron
534 Homeostasis of Its Microbiota Partner *Aspergillus Fumigatus* via Phenazines. *Sci. Rep.*
535 **2015**, *5*, 8220.
- 536 (28) Wang, Y.; Newman, D. K. Redox Reactions of Phenazine Antibiotics with Ferric
537 (hydr)oxides and Molecular Oxygen. *Environ. Sci. Technol.* **2008**, *42* (7), 2380–2386.
- 538 (29) Ramos, I.; Dietrich, L. E. P.; Price-Whelan, A.; Newman, D. K. Phenazines Affect Biofilm
539 Formation by *Pseudomonas Aeruginosa* in Similar Ways at Various Scales. *Res.*
540 *Microbiol.* **2010**, *161* (3), 187–191.
- 541 (30) Hofmann, A. F.; Eckmann, L. How Bile Acids Confer Gut Mucosal Protection against
542 Bacteria. *Proc. Natl. Acad. Sci. U. S. A.* **2006**, *103* (12), 4333–4334.
- 543 (31) Cleary, J. L.; Condren, A. R.; Zink, K. E.; Sanchez, L. M. Calling All Hosts: Bacterial
544 Communication in Situ. *Chem* **2017**, *2* (3), 334–358.
- 545 (32) Galey, M. M.; Sanchez, L. M. Spatial Analyses of Specialized Metabolites: The Key to
546 Studying Function in Hosts. *mSystems* **2018**, *3* (2).
547 <https://doi.org/10.1128/mSystems.00148-17>.
- 548 (33) Sakhtah, H.; Koyama, L.; Zhang, Y.; Morales, D. K.; Fields, B. L.; Price-Whelan, A.;
549 Hogan, D. A.; Shepard, K.; Dietrich, L. E. P. The *Pseudomonas Aeruginosa* Efflux Pump
550 MexGHI-OpmD Transports a Natural Phenazine That Controls Gene Expression and
551 Biofilm Development. *Proc. Natl. Acad. Sci. U. S. A.* **2016**, *113* (25), E3538–E3547.
- 552 (34) Filkins, L. M.; Graber, J. A.; Olson, D. G.; Dolben, E. L.; Lynd, L. R.; Bhujju, S.; O’Toole,
553 G. A. Coculture of *Staphylococcus Aureus* with *Pseudomonas Aeruginosa* Drives *S.*
554 *Aureus* towards Fermentative Metabolism and Reduced Viability in a Cystic Fibrosis
555 Model. *J. Bacteriol.* **2015**, *197* (14), 2252–2264.
- 556 (35) Phelan, V. V.; Moree, W. J.; Aguilar, J.; Cornett, D. S.; Koumoutsis, A.; Noble, S. M.;
557 Pogliano, K.; Guerrero, C. A.; Dorrestein, P. C. Impact of a Transposon Insertion in
558 *phzF2* on the Specialized Metabolite Production and Interkingdom Interactions of
559 *Pseudomonas Aeruginosa*. *J. Bacteriol.* **2014**, *196* (9), 1683–1693.
- 560 (36) Machan, Z. A.; Taylor, G. W.; Pitt, T. L.; Cole, P. J.; Wilson, R. 2-Heptyl-4-
561 Hydroxyquinoline N-Oxide, an Antistaphylococcal Agent Produced by *Pseudomonas*
562 *Aeruginosa*. *J. Antimicrob. Chemother.* **1992**, *30* (5), 615–623.
- 563 (37) Hoffman, L. R.; Déziel, E.; D’Argenio, D. A.; Lépine, F.; Emerson, J.; McNamara, S.;
564 Gibson, R. L.; Ramsey, B. W.; Miller, S. I. Selection for *Staphylococcus Aureus* Small-
565 Colony Variants due to Growth in the Presence of *Pseudomonas Aeruginosa*. *Proc. Natl.*
566 *Acad. Sci. U. S. A.* **2006**, *103* (52), 19890–19895.
- 567 (38) Biswas, L.; Biswas, R.; Schlag, M.; Bertram, R.; Götz, F. Small-Colony Variant Selection
568 as a Survival Strategy for *Staphylococcus Aureus* in the Presence of *Pseudomonas*
569 *Aeruginosa*. *Appl. Environ. Microbiol.* **2009**, *75* (21), 6910–6912.
- 570 (39) Voggu, L.; Schlag, S.; Biswas, R.; Rosenstein, R.; Rausch, C.; Götz, F. Microevolution of
571 Cytochrome *Bd* Oxidase in *Staphylococci* and Its Implication in Resistance to

- 572 Respiratory Toxins Released by Pseudomonas. *J. Bacteriol.* **2006**, *188* (23), 8079–8086.
- 573 (40) Kim, K.; Kim, Y. U.; Koh, B. H.; Hwang, S. S.; Kim, S.-H.; Lépine, F.; Cho, Y.-H.; Lee, G.
- 574 R. HHQ and PQS, Two Pseudomonas Aeruginosa Quorum-Sensing Molecules, down-
- 575 Regulate the Innate Immune Responses through the Nuclear Factor-kappaB Pathway.
- 576 *Immunology* **2010**, *129* (4), 578–588.
- 577 (41) Häussler, S.; Becker, T. The Pseudomonas Quinolone Signal (PQS) Balances Life and
- 578 Death in Pseudomonas Aeruginosa Populations. *PLoS Pathog.* **2008**, *4* (9), e1000166.
- 579 (42) Gallagher, L. A.; McKnight, S. L.; Kuznetsova, M. S.; Pesci, E. C.; Manoil, C. Functions
- 580 Required for Extracellular Quinolone Signaling by Pseudomonas Aeruginosa. *J.*
- 581 *Bacteriol.* **2002**, *184* (23), 6472–6480.
- 582 (43) Donlan, R. M. Biofilms: Microbial Life on Surfaces. *Emerg. Infect. Dis.* **2002**, *8* (9), 881–
- 583 890.
- 584 (44) Cornelis, P.; Dingemans, J. Pseudomonas Aeruginosa Adapts Its Iron Uptake Strategies
- 585 in Function of the Type of Infections. *Front. Cell. Infect. Microbiol.* **2013**, *3*, 75.
- 586 (45) Diggle, S. P.; Matthijs, S.; Wright, V. J.; Fletcher, M. P.; Chhabra, S. R.; Lamont, I. L.;
- 587 Kong, X.; Hider, R. C.; Cornelis, P.; Cámara, M.; et al. The Pseudomonas Aeruginosa 4-
- 588 Quinolone Signal Molecules HHQ and PQS Play Multifunctional Roles in Quorum
- 589 Sensing and Iron Entrapment. *Chem. Biol.* **2007**, *14* (1), 87–96.
- 590 (46) Kang, D.; Kirienko, D. R.; Webster, P.; Fisher, A. L.; Kirienko, N. V. Pyoverdine, a
- 591 Siderophore from Pseudomonas Aeruginosa, Translocates into C. Elegans, Removes
- 592 Iron, and Activates a Distinct Host Response. *Virulence* **2018**, *9* (1), 804–817.
- 593 (47) Cox, C. D. Effect of Pyochelin on the Virulence of Pseudomonas Aeruginosa. *Infect.*
- 594 *Immun.* **1982**, *36* (1), 17–23.
- 595 (48) Lépine, F.; Milot, S.; Déziel, E.; He, J.; Rahme, L. G. Electrospray/mass Spectrometric
- 596 Identification and Analysis of 4-Hydroxy-2-Alkylquinolines (HAQs) Produced by
- 597 Pseudomonas Aeruginosa. *J. Am. Soc. Mass Spectrom.* **2004**, *15* (6), 862–869.
- 598 (49) Bredenbruch, F.; Nimtz, M.; Wray, V.; Morr, M.; Müller, R.; Häussler, S. Biosynthetic
- 599 Pathway of Pseudomonas Aeruginosa 4-Hydroxy-2-Alkylquinolines. *J. Bacteriol.* **2005**,
- 600 *187* (11), 3630–3635.
- 601 (50) Wang, Y.; Wilks, J. C.; Danhorn, T.; Ramos, I.; Croal, L.; Newman, D. K. Phenazine-1-
- 602 Carboxylic Acid Promotes Bacterial Biofilm Development via Ferrous Iron Acquisition. *J.*
- 603 *Bacteriol.* **2011**, *193* (14), 3606–3617.
- 604 (51) Dow, J. M.; Crossman, L.; Findlay, K.; He, Y.-Q.; Feng, J.-X.; Tang, J.-L. Biofilm
- 605 Dispersal in Xanthomonas Campestris Is Controlled by Cell-Cell Signaling and Is
- 606 Required for Full Virulence to Plants. *Proc. Natl. Acad. Sci. U. S. A.* **2003**, *100* (19),
- 607 10995–11000.
- 608 (52) Rossmann, F. S.; Racek, T.; Wobser, D.; Puchalka, J.; Rabener, E. M.; Reiger, M.;
- 609 Hendrickx, A. P. A.; Diederich, A.-K.; Jung, K.; Klein, C.; et al. Phage-Mediated
- 610 Dispersal of Biofilm and Distribution of Bacterial Virulence Genes Is Induced by Quorum
- 611 Sensing. *PLoS Pathog.* **2015**, *11* (2), e1004653.
- 612 (53) Uppuluri, P.; Chaturvedi, A. K.; Srinivasan, A.; Banerjee, M.; Ramasubramaniam, A. K.;
- 613 Köhler, J. R.; Kadosh, D.; Lopez-Ribot, J. L. Dispersion as an Important Step in the
- 614 Candida Albicans Biofilm Developmental Cycle. *PLoS Pathog.* **2010**, *6* (3), e1000828.
- 615 (54) Hay, A. J.; Zhu, J. Host Intestinal Signal-Promoted Biofilm Dispersal Induces Vibrio
- 616 Cholerae Colonization. *Infect. Immun.* **2015**, *83* (1), 317–323.
- 617 (55) Connolly, K. L.; Roberts, A. L.; Holder, R. C.; Reid, S. D. Dispersal of Group A
- 618 Streptococcal Biofilms by the Cysteine Protease SpeB Leads to Increased Disease
- 619 Severity in a Murine Model. *PLoS One* **2011**, *6* (4), e18984.
- 620 (56) Desbois, A. P.; Coote, P. J. Wax Moth Larva (Galleria Mellonella): An in Vivo Model for
- 621 Assessing the Efficacy of Antistaphylococcal Agents. *J. Antimicrob. Chemother.* **2011**,
- 622 *66* (8), 1785–1790.

- 623 (57) Kaplan, E. L.; Meier, P. Nonparametric Estimation from Incomplete Observations. *J. Am.*
624 *Stat. Assoc.* **1958**, 53 (282), 457–481.
- 625 (58) Bland, J. M.; Altman, D. G. The Logrank Test. *BMJ* **2004**, 328 (7447), 1073.
- 626 (59) Benjamini, Y.; Hochberg, Y. Controlling the False Discovery Rate: A Practical and
627 Powerful Approach to Multiple Testing. *J. R. Stat. Soc. Series B Stat. Methodol.* **1995**,
628 57 (1), 289–300.
- 629 (60) Adler, C.; Corbalán, N. S.; Seyedsayamdost, M. R.; Pomares, M. F.; de Cristóbal, R. E.;
630 Clardy, J.; Kolter, R.; Vincent, P. A. Catecholate Siderophores Protect Bacteria from
631 Pyochelin Toxicity. *PLoS One* **2012**, 7 (10), e46754.

632